

# Unusual major stratospheric sudden warming event from January to February 2009

## 1. Introduction

A major stratospheric sudden warming (SSW) event began in January 2009. This report outlines analysis of the atmospheric circulation during the event using the Japan Meteorological Agency (JMA) Climate Data Assimilation System (JCDAS).

In winter, JMA's Climate Prediction Division (CPD) monitors stratospheric circulation in the Northern Hemisphere. When an SSW occurs, JMA begins to issue stratospheric alerts (known as STRAT-ALERT reports) via the Global Telecommunication System (GTS). According to the World Meteorological Organization (WMO) definition, a minor SSW is identified when polar temperatures increase by 25 K or more within a week at any stratospheric level. If the zonal mean temperature increases in the polar region and net zonal mean zonal winds become easterly to the north of 60°N at 10 hPa or below, the event is classified as a major SSW.

## 2. Data and Methods

JMA used six-hourly reanalysis datasets produced from both the Japanese 25-year Reanalysis Project (JRA-25) and JCDAS, which succeeds the system of the JRA-25 project for near-real-time climate monitoring. The global model used in JRA-25 has a spectral resolution equivalent to a horizontal grid size of around 120 km (T106) and 40 vertical layers, with the top level at 0.4 hPa. The details of JRA-25, which covers the 26-year period from 1979 to 2004, can be referred to in Onogi et al. (2007). In this study, the daily climatological means were calculated from 1979 to 2004 and smoothed using a 60-day low-pass filter (Duchon, 1979).

Wave activity flux indicates the direction of a Rossby wave packet propagation in three-dimensional space, and these values were calculated based on Plumb (1985). The results are quite useful in analyzing the passage of Rossby waves propagating from the troposphere to the stratosphere.

In the zonal mean field, Eliassen Palm flux (EP flux) is used to diagnose eddy forcing of the basic flow as well as to provide a direct view of the westerly momentum transport processes (Palmer, 1982). EP flux also represents the direction of an eddy's energy propagation in the zonal mean field, and its horizontal and vertical components represent meridional westward momentum transport and heat transport by eddies, respectively. In addition, the total eddy forcing of the basic flow can be represented by the divergence (i.e., the acceleration of westerly winds) and convergence (the deceleration of westerly winds) of EP flux.

## 3. Results

The zonal wind speed and temperature at the 10-hPa level in the zonal mean field during the winter of 2008/2009 are shown in Fig. 1. In early January, the axis of the polar night jet was located at around 65°N. The air temperature in the polar region was around 200 K. Subsequently, a poleward shift of the polar night jet was observed along with a rapid increase in air temperature, which exceeded 265 K at the 10-hPa level by mid-January, and the CPD began to issue STRAT-ALERT reports for a minor SSW. Then, zonal winds reversed from westerlies to

easterlies in the mid-latitudes, and easterlies expanded from 50°N to the North Pole. Figures 2a and 2b show time-height cross sections of zonal mean temperature and its anomalies averaged over 75° – 90°N and of zonal mean zonal wind and its anomalies at 60°N, respectively. At the beginning of this major SSW event, the increase in temperature and the reversed zonal wind direction were limited to the area above the middle stratosphere. The polar vortex split clearly into two in late January (shown later), and the reversed zonal wind direction was observed throughout the stratosphere to the north of 60°N in early February. Accordingly, this event was identified as a major SSW in line with WMO’s classification. A poleward increase in temperature was clearly observed to the north of 60°N (Fig. 1). Consequently, the reverse of zonal mean zonal winds continued until the end of February 2009.

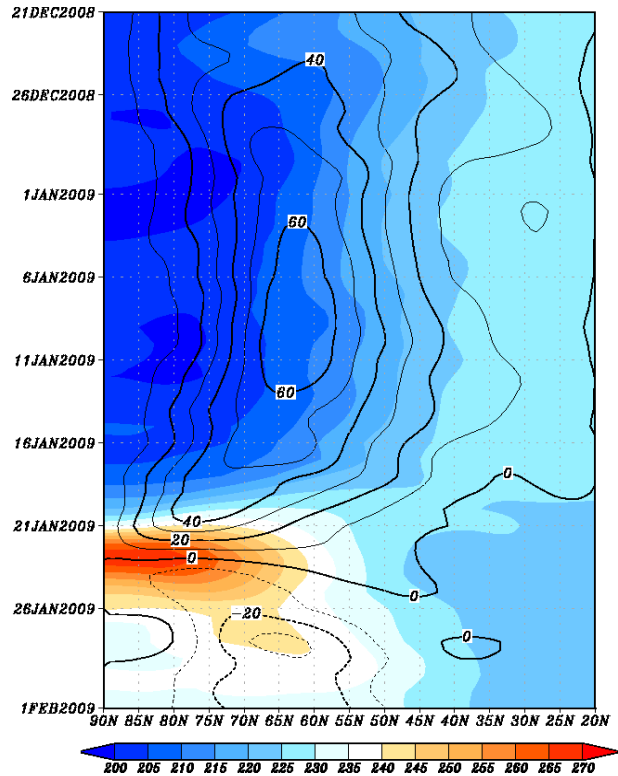


Figure 1. Latitude-time cross section of 10-hPa zonal mean zonal wind (contours) and temperature (shaded). The contour interval is 10 ms<sup>-1</sup>.

Figure 2c shows a time series of the vertical component of EP flux averaged over 30° – 90°N at the 100-hPa level. In early January, upward propagation of the planetary wave was below the climatological mean. In mid-January, the vertical component of EP flux for the planetary wave of zonal wave number 2 began to sharply increase, and peaked on 19 January. Conversely, only a slight increase was observed in the vertical component of EP flux for zonal waves 1 and 3, which indicates that the energy of zonal wave number 2 was dominant among planetary waves during MSSWJ09. Figure 2d shows a time-height cross section of the vertical component of EP flux averaged over 30° – 90°N for the planetary wave of zonal wave number 2. In mid-January, the vertical component of EP flux began to increase in the troposphere. It also increased in the stratosphere within a few days and peaked within a week. This means that it took less than a week for the energy of the planetary wave of zonal wave number 2 to propagate upward from the troposphere to the stratosphere. After the peak in the stratosphere, the region in which the vertical component of EP flux exceeded 4 m<sup>2</sup>s<sup>-2</sup> gradually descended toward the lower stratosphere from late January to early February, and disappeared throughout the stratosphere in the second half of February. Comparing Figs. 2a and 2b with Fig. 2c, it can be seen that both the temperature increase and the easterly winds were observed just after the peak of the upward propagation of the planetary waves for zonal wave number 2, and that the strong upward propagation was generally limited to the westerly region.

Figure 3 shows the annual variability of each zonal wave number to the sum of zonal waves 1 and 2 in the winter total amount of the vertical component of EP flux at the 100-hPa level averaged

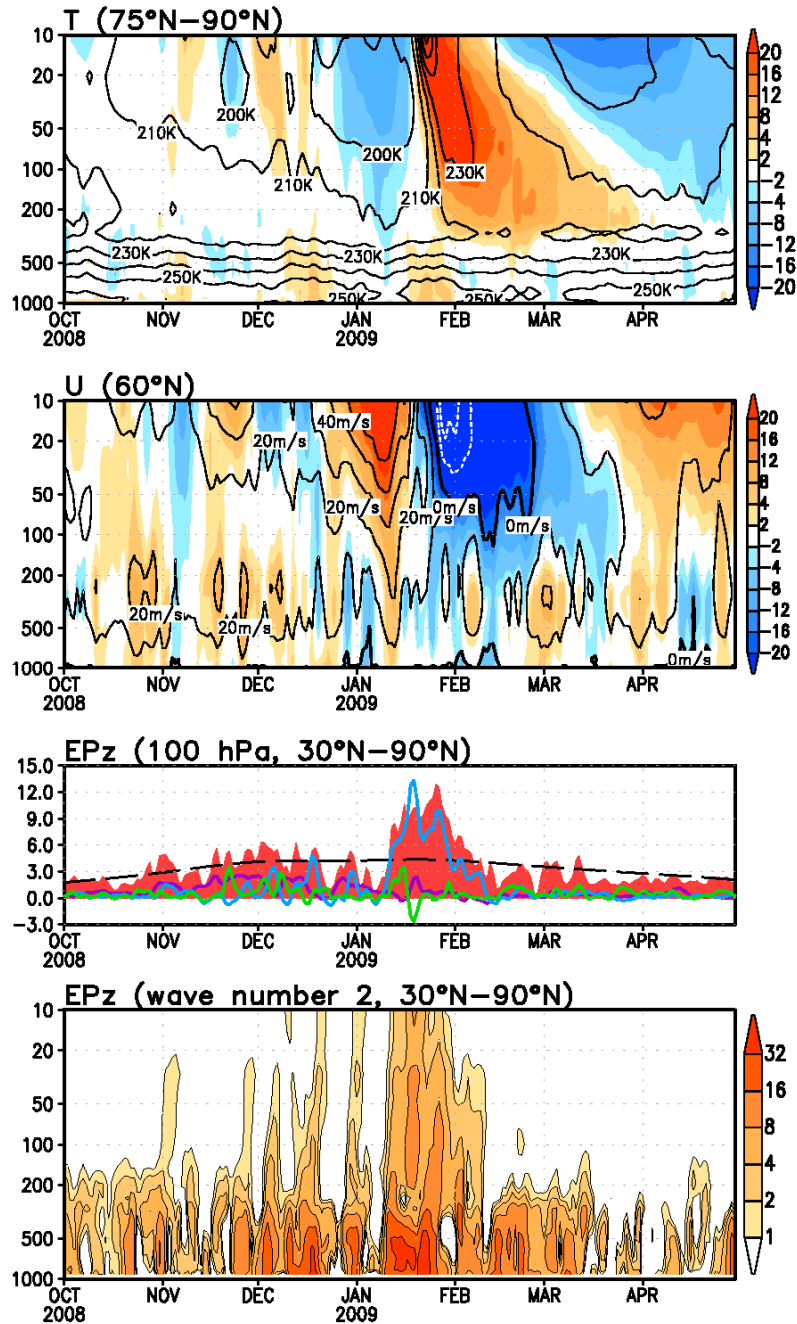


Figure 2. (a) Time-height cross sections of zonal mean temperature (contours) and its deviation from the climatological mean (shaded) averaged over 75° – 90°N, (b) time-height cross sections of zonal mean zonal wind (contours) and its deviation from the climatological mean (shaded) at 60°N, (c) time series of the vertical component of EP flux averaged over 30° – 90°N at the 100-hPa level, and (d) time-height cross sections of the vertical component of EP flux for zonal wave number 2 averaged over 30° – 90°N. The contour intervals are (a) 10 K and (b) 5  $ms^{-1}$ , respectively. The red bars in (c) denote the vertical component of EP flux for whole zonal wave numbers. The purple, light-green and light-blue lines denote the vertical components of EP flux for zonal waves 1, 2 and 3, respectively. The broken line in (c) denotes the climatological mean for the vertical component of EP flux for whole zonal wave numbers. The unit of the vertical component for EP flux in (c) and (d) is  $m^2s^{-2}$ .

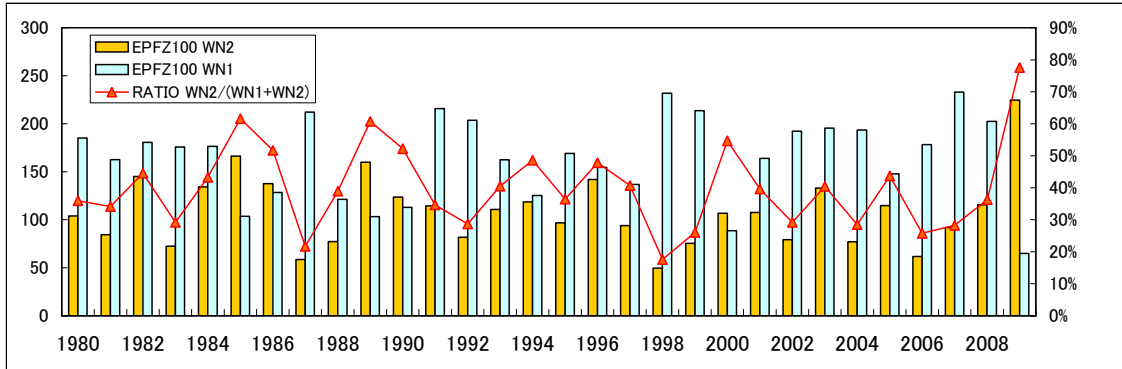


Figure 3. Annual variability in the total vertical component of EP flux at the 100-hPa level averaged over 30° – 90°N during boreal winter (Dec. – Feb.). The yellow and light-blue bars denote the ratio of the seasonal total amounts of the vertical component of EP flux ( $\text{m}^2\text{s}^{-2}$ ) for zonal waves 1 and 2, respectively. The line in the graph denotes the values for the ratio of zonal wave number 2 to the sum of zonal waves 1 and 2.

over 30° – 90°N. The ratios of the vertical component of EP flux for zonal wave number 2 have exceeded 60% only in the three winters of 1984/85, 1988/89 and 2008/09. In addition, it is noteworthy that the ratio for the planetary wave of zonal wave number 2 during winter 2008/09 was the highest among the past 30 winters. This was extraordinary because the normalized value of the deviation from its climatological mean exceeded  $4\sigma$ . According to Charlton and Polvani as well as the results of CPD/JMA analysis, 22 cases of major sudden stratospheric warming in boreal mid-winter have been analyzed over the past 31 winters. We investigated the zonal wave number that contributed most to SSW events using this past data, and found that the majority were caused by the planetary wave of zonal wave number 1. It can be concluded that MSSWJ09 provides the most prominent discovery in terms of the energy of the planetary wave of zonal wave number 2.

Here, we outline atmospheric circulation during the MSSWJ09 event. Figure 4 shows 10-hPa geopotential heights and their deviation from the zonal mean (top panels) and longitude-height cross sections of geopotential height deviations, temperature deviations and Plumb's wave activity fluxes averaged over 50° – 70°N (bottom panels) for selected five-day means. During the period prior to MSSWJ09 (Fig. 4a), the polar vortex was located over the North Pole. A westward tilt with height was found only over Europe, where only a weak upward propagation of the planetary wave was seen. During the first developmental stage (Fig. 4b), geopotential height deviations corresponding to the development of a planetary wave of zonal wave number 2 became clear, and the polar vortex began to split into two vortices. One of these was located over the Taimyr Peninsula, and the other was located over Baffin Island. The geopotential height field in the stratosphere clearly shows the westward tilt with height, which indicates the upward propagation of wave activity. Remarkable planetary wave packets emanated from a ridge over the Alaska Peninsula and propagated over the North Atlantic in the stratosphere. Part of these planetary wave packets propagated along both the tropospheric polar front jet and the subtropical jet, reaching and strengthening a trough over central

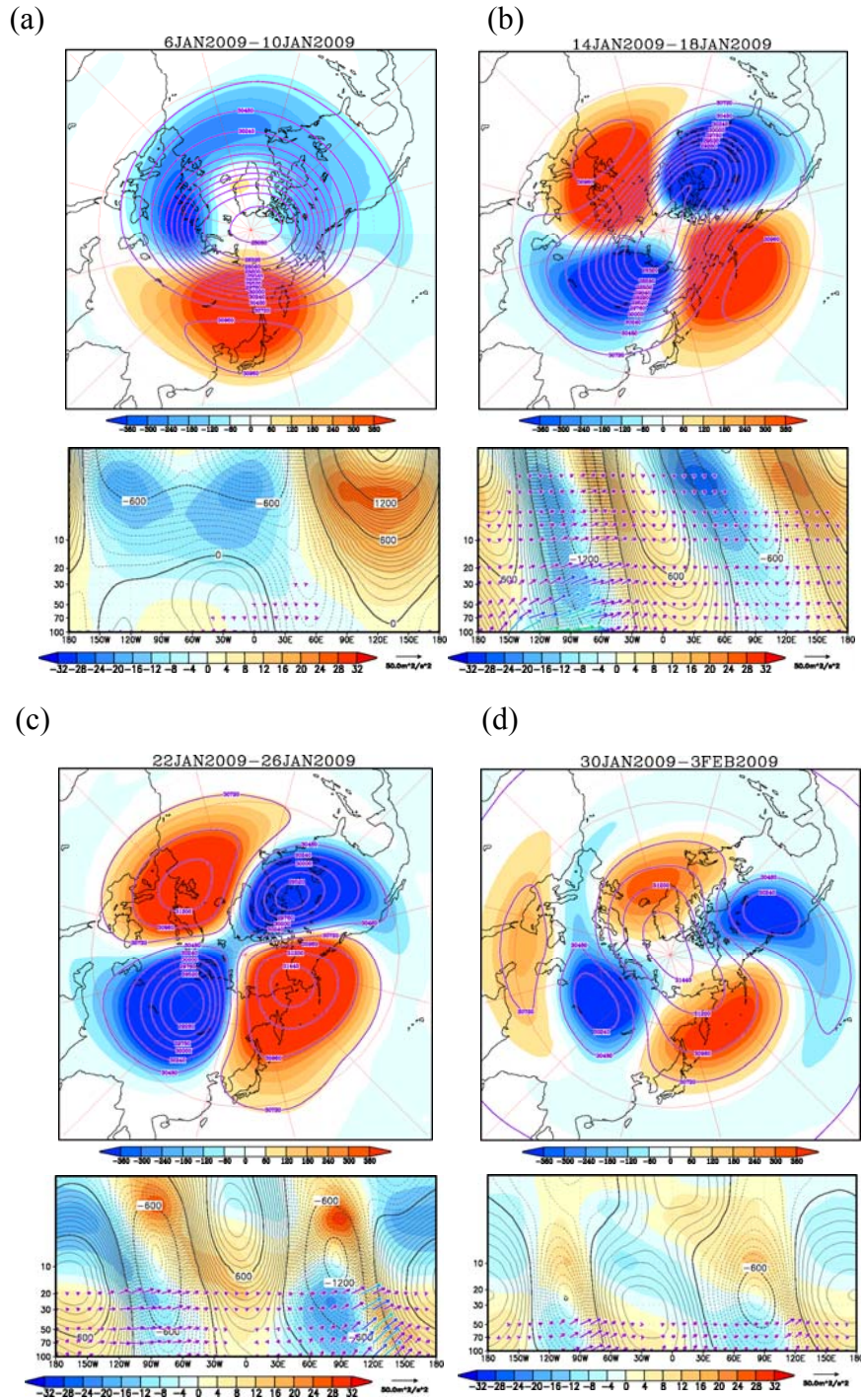


Figure 4. (Top) 10-hPa geopotential height (contours) and deviations from the zonal mean (shaded), and (bottom) longitude-height cross sections of height deviations from the zonal mean (contours) and Plumb's wave activity flux (vectors) in the stratosphere from 100 to 1 hPa averaged over  $50^{\circ} - 70^{\circ}\text{N}$  for selected five-day means. The contour intervals are 240 m (top panels) and 60 m (bottom panels). The unit of Plumb's wave activity flux is  $\text{m}^2\text{s}^{-2}$ . (a), (b), (c) and (d) denote the means for 6 – 10 January, 14 – 18 January, 22 – 26 January and 30 January – 3 February, respectively.

Siberia (not shown). Moreover, these wave packets propagated upward into the stratosphere, although they were restricted to the lower stratosphere during the second developmental stage (Fig. 4c). The Aleutian high developed in the stratosphere, and the two polar vortices shifted southwestward. The development of the Aleutian high was observed below the 10-hPa level, but the westward tilt of the geopotential height deviation was not clear. It can be said that the planetary wave packets emanating from the trough over central Siberia appeared to be crucial for the polar vortex split. During the mature stage (Fig. 4d), the two polar vortices completely split into two, and the upward propagation of the planetary wave packets weakened. The two vortices gradually lost strength until mid-February.

Here, we describe the characteristics of atmospheric circulation in the troposphere during the first developmental stage of SSW09. Figure 5 shows (a) 250-hPa Plumb's wave activity flux, geopotential height and its deviation from the zonal mean, (b) longitude-height cross section of Plumb's wave activity flux and geopotential height deviation from the zonal mean for 12 – 16 January. A ridge developed remarkably over Alaska in the upper troposphere (Fig. 5a) due to wave packets emanating from a synoptic-scale disturbance in the lower troposphere in the North Pacific (not shown).

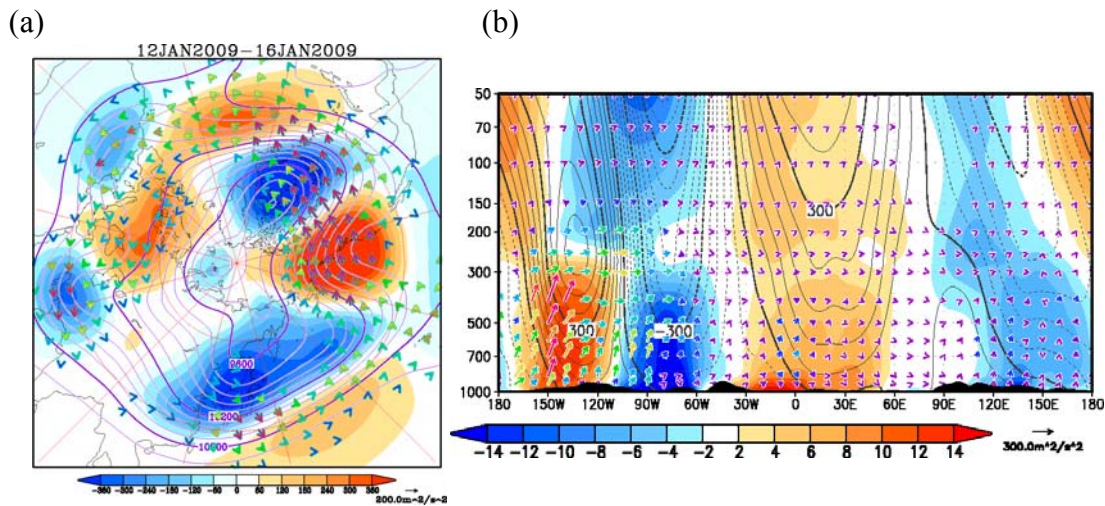


Figure 5. (a) 250-hPa Plumb's wave activity flux (vectors), geopotential height (contours) and its deviation from the climatological mean (shaded), and (b) longitude-height cross section of geopotential height deviations from the zonal mean (contours), temperature deviations from the zonal mean (shaded) and Plumb's wave activity flux (vector) averaged over 50° – 70°N in the troposphere and the lower stratosphere from 1,000 to 50 hPa averaged for 12 – 16 January 2009. The contour intervals in (a) and (b) are 60 m and 10 m, respectively. The unit of Plumb's wave activity flux is  $\text{m}^2\text{s}^{-2}$ .

#### 4. Summary

The major characteristics of this SSW event can be summarized as follows:

First, the planetary wave of zonal wave number 2 was dominant during this SSW. We found that the total amount of energy propagated by this planetary wave from the troposphere to the stratosphere was the strongest since winter 1979/80. This was extraordinary because the

normalized value of the deviation from its climatological mean exceeded  $4\sigma$ . This SSW represents the most prominent discovery in terms of the energy of the planetary wave of zonal wave number 2.

Second, the development of a ridge over Alaska played an important role in the development of the planetary wave, as this ridge emanated strong Rossby wave packets toward the eastern part of North America and was related to the intensification of the tropospheric polar front jet at the beginning of this SSW. Moreover, during the first developmental stage of MSSWJ09, part of the strong planetary wave packets directly propagated from the troposphere to the stratosphere, as shown in the bottom panels of Fig. 4b (from 100 to 1 hPa) and Fig. 5b (from 1,000 to 50 hPa). During the second developmental stage of MSSWJ09, part of the wave packets emanating from the ridge over Alaska propagated along the sub-tropical jet in the upper troposphere and moved upward toward the stratosphere over central Siberia. These wave packets were crucial for the polar vortex split.

### References

- Duchon, C. E., 1979: Lanczos filtering in one and two dimensions. *J. Applied Meteor.*, 18, 1016-1022.
- Onogi, K., J. Tsutsui, H. Koide, M. Sakamoto, S. Kobayashi, H. Hatsushika, T. Matsumoto, N. Yamazaki, H. Kamahori, K. Takahashi, S. Kadokura, K. Wada, K. Kato, R. Oyama, T. Ose, N. Mannoji and R. Taira, 2007: The JRA-25 Reanalysis. *J. Meteor. Soc. Japan*, 85, 369-432.
- Palmer, T. N., 1982: Properties of the Eliassen-Palm flux for planetary scale motions. *J. Atmos. Sci.*, 39, 992-997.
- Plumb, R. A., 1985: On the three dimensional propagation of stationary waves. *J. Atmos. Sci.*, 42, 217-229.